Inorganic Chemistry

Article

pubs.acs.org/IC

Chiral Conducting Salts of Nickel Dithiolene Complexes

Julien Lieffrig,[†] Olivier Jeannin,[†] Pascale Auban-Senzier,[‡] and Marc Fourmigué*[,†]

[†]Sciences Chimiques de Rennes, Université Rennes 1 and CNRS UMR 6226, Campus de Beaulieu, 35042 Rennes, France

[‡]Laboratoire de Physique des Solides, Université Paris Sud, CNRS, UMR 8502, 91405 Orsay, France

Supporting Information

ABSTRACT: Conducting and chiral $[Ni(dmit)_2]$ dithiolene salts were obtained by electrocrystallization of the radical $[n\text{-}Bu_4N][Ni(dmit)_2]$ salt in the presence of chiral, enantiopure trimethylammonium cations. Three different cations were investigated, namely, (*R*)-Ph(Me)HC*-NMe_3^+, (*S*)-(^{t}Bu)(Me)HC*-NMe_3^+, and (*S*)-(1-Napht)MeHC*-NMe_3^+, noted (*R*)-**1**, (*S*)-**2**, and (*S*)-**3**. Salts of 1:3 stoichiometry were obtained with (*R*)-**1** and (*S*)-**2**, formulated as $[(R)\text{-}\mathbf{1}][Ni(dmit)_2]_3$ and $[(S)\text{-}\mathbf{2}][Ni(dmit)_2]_3{\cdot}(CH_3CN)_2$. They both crystallize in the $P2_12_12_1$ chiral space group, with three crystallographically independent complexes exhibiting different oxidation degrees. Another salt with 2:5 stoichiometry was isolated with (*S*)-**3**. The semiconducting character of the three salts (σ_{RT} = 20−30 × 10^{-3} S cm^{-1}) finds its origin in a strong electron localization, favored by the large number of crystallographically independent $[Ni(dmit)_2]$ complexes in these chiral structures and their association into weakly interacting dimeric or trimeric motifs. Racemic salts with the same cations, obtained only with difficulties with the *tert*-butyl-containing (*rac*)-**2** cation, afforded similar trimerized structures. The observed unusual stoichiometry and strong charge localization is tentatively assigned to the size and anisotropic charge distribution of the cations.

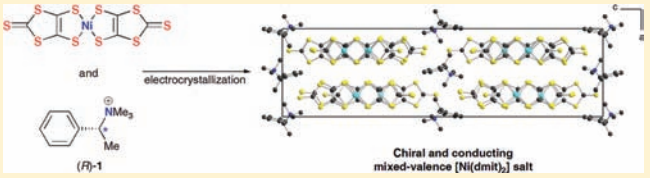

INTRODUCTION

The combination of conductivity and chirality is currently being investigated by several groups around the world, particularly aiming at observation of so-called magneto-chiral effects of the conductivity, as predicted and already observed by Rikken in chiral nanotubes.[1] Molecular conductors are particularly attractive for controlled introduction of chirality, and several strategies were considered to reach this goal. As the broadest family of organic conductors is based on cation radical salts of donor molecules such as tetrathiafulvalenes, the chirality was effectively introduced in those salts,[2,3] either on the TTF core itself or on the counterion. The first approach already started in 1986 with methyl derivatives of BEDT-TTF,[4,5] and several conducting salts were successfully obtained.[6,7] Tetrathiafulvalenes substituted with chiral oxazolines were also investigated[8] and afforded several series of (*R*)-, (*S*)-, and racemic salts with metallic conductivity.[9] This concept was recently extended to TTF derivatives with axial chirality introduced by binaphthol moieties.[10] The second approach involving chiral counterions was investigated with $M^{III}(oxalate)_3$,[11] $Fe(croconate)_3$,[12] $[M^{III}(S,S\text{-EDDS})]$ (EDDS = ethylenediaminedisuccinato),[13] Sb_2(L-tartrate)$_2$,[14] TRISPHAT,[15] or organic anions such as D-camphorsulfonate[16] in electrocrystallization experiments. A third original approach to chiral cation radical salts involves use of a neutral chiral solvent molecule able to either intersperse within the anionic layer and/or favor one enantiomer within a racemic mixture.[17]

All examples reported above involve exclusively cation radical salts derived from TTF-based donor molecules. However, another broad family of molecular conductors is also found among the partially oxidized $[M(dithiolene)_2]^-$ complexes with M = Ni, Pd, Pt.[18] Indeed, electrocrystallization of the radical anion species $[M(dithiolene)_2]^-$ can afford mixed-valence salts formulated as $C[M(dithiolene)_2]_2$, where C^+ can be a closed- or open-shell radical. Examples of superconducting salts are found with $[Ni(dmit)_2]^-$ together with $TTF^{+\bullet}$,[19] or EDT-$TTF^{+\bullet}$ radical cations,[20] or $[Pd(dmit)_2]^-$ with small closed-shell cations such as Me_4N^+, Me_4As^+, and Me_4Sb^+ or larger $Et_2Me_2N^+$ and $Et_2Me_2P^+$.[21] Another remarkable result within these series is identification of a quantum spin liquid (QSL) ground state within the series of stibonium salts.[22] Introduction of chirality within such dithiole-based conducting salts has never been considered, albeit it can potentially be done in two ways as illustrated above with TTFs, that is, (i) dithiolene complexes with chiral substituents and (ii) electrocrystallization of achiral dithiolene complexes such as $[M(dmit)_2]^-$ in the presence of chiral cations. Only a few examples of dithiolene complexes with chiral substituents were reported to date, a radical anion cocrystallized with chiral viologens,[23] several neutral nickel dithiolene complexes capable of inducing a chiral nematic phase when dissolved into a nematic liquid crystal host,[24] and, more recently, Ni and Au dithiolene complexes derived from camphordione.[25] The second route based on achiral dithiolene complexes partially oxidized in the presence of chiral cations was not investigated so far.

We report here the first examples of conducting chiral salts of $[Ni(dmit)_2]^-$ dithiolene complexes with, as counterions, chiral cations such as (*R*)-Ph(Me)HC*-NMe_3^+,[26] (*S*)-(^{t}Bu)(Me)-HC*-NMe_3^+, and (*S*)-(1-Napht)MeHC*-NMe_3^+. We describe

Received: January 19, 2012
Published: February 29, 2012

   dx.doi.org/10.1021/ic300146s | *Inorg. Chem.* 2012, 51, 7144−7152

their syntheses, X-ray crystal structures, and transport properties in relationship with the chiral nature of the counterion. Of particular interest is the unusual stoichiometries obtained recurrently within these series with a cation to complex ratio of 1:3 and 2:5, at variance with the most common 1:2 stoichiometry, associated with a recurrent charge localization. When possible, comparison with the racemic salts will be also conducted.

RESULTS AND DISCUSSION

Crystallization of the chiral mixed-valence conducting dithiolene salts of $[Ni(dmit)_2]^-$ is based on the electrocrystallization of its nBu_4N^+ salt, $(nBu_4N)[Ni(dmit)_2]$, in the presence of a large excess of the chiral cation as electrolyte. Under such conditions, we hope to crystallize a salt incorporating the desired cation rather than the only known mixed-valence salt with nBu_4N^+, $(nBu_4N)_2[Ni(dmit)_2]_7\cdot(CH_3CN)_2$.[27] As described by Lacour,[28] the chiral cations were prepared by MeI alkylation of the commercially available primary amines, (*R*)-Ph(Me)C*H-NH_2, (*S*)-(^{t}Bu)(Me)C*H-NH_2, and (*S*)-(1-Napht)MeC*H-NH_2, affording the corresponding iodide salts, (*R*)-Ph(Me)C*H-NMe_3I, (*S*)-(^{t}Bu)(Me)C*H-NMe_3I, and (*S*)-(1-Napht)MeC*H-NMe_3I. Metathesis with HPF_6 in water/MeOH allowed for isolation of the hexafluorophosphate salts, noted, respectively, [(*R*)-**1**,PF_6], [(*S*)-**2**,PF_6], and [(*S*)-**3**,PF_6] in the following.

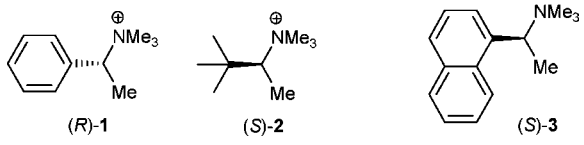

Electrocrystallization of $[nBu_4N][Ni(dmit)_2]$ in the presence of the phenyl cationic derivative (*R*)-**1** as electrolyte afforded a salt formulated as $[(R)\text{-}\mathbf{1}][Ni(dmit)_2]_3$ with 1:3 stoichiometry, which crystallizes in the orthorhombic system, space group (chiral) $P2_12_12_1$, with one cation and three $[Ni(dmit)_2]$ species in general position in the unit cell. Intramolecular bond lengths within the three independent complexes are collected in Table 1 and indicate that the three complexes do not have the same charge. Indeed, the HOMO of closed-shell reduced $[Ni(dmit)_2]^{2-}$ has, within the metallacycles, a bonding character for the C=C bond and an antibonding character for the C−S and Ni−S bond. As a consequence, more oxidized species exhibit a lengthening of the C=C bond with concomitant shortening of the C−S and Ni−S bonds. Examination of Table 1 shows that complex Ni(3) is essentially neutral while the two other share the −1 charge, with Ni(2) possibly slightly more oxidized than Ni(1)

As shown in Figure 1, the partially oxidized dithiolene complexes are organized into layers, separated from each other by the chiral enantiopure cations. Note also a short S···S interlayer contact (dotted lines in Figure 1) at 3.392(2) Å. The complexes stack along the *b* axis (Figure 2), with three different overlap interactions, an almost eclipsed one for Ni(1)−Ni(2) and more distorted ones for the Ni(1)−Ni(3) and Ni(2)−Ni(3) overlap. Calculations of the $\beta_{LUMO-LUMO}$ interaction energies for the three Ni(1)−Ni(2), Ni(2)−Ni(3), and (Ni1)−Ni(3) pairs of $[Ni(dmit)_2]$ complexes confirm this observation, with β_{12} = 0.51 eV, while β_{23} = 0.09 and β_{13} = 0.005 eV. Combined with the charge distribution detailed above, this salt thus appears as mixed-valence $[Ni(1)-Ni(2)]^{-1}$ dyads,

Table 1. Average Intramolecular Bond Distances Within the $[Ni(dmit)_2]$ Metallacycles in the Different Salts and Reference Compounds

	Ni−S (Å)	S−C (Å)	C=C (Å)	ref
reference compds				
$[Ni(dmit)_2]^{-2}$ [a]	2.195(9)	1.733(8)	1.352(3)	29
$[Ni(dmit)_2]^{-}$ [a]	2.166(10)	1.715(10)	1.360(6)	30
$[Ni(dmit)_2]^{-0.5}$ [b]	2.163(3)	1.701(4)	1.382(7)	31
$[Ni(dmit)_2]^{0}$	2.143(3)	1.698(5)	1.393(10)	32
with (*R*)-**1**				
Ni(1)	2.165(2)	1.717(6)	1.381(8)	this work
Ni(2)	2.162(2)	1.706(6)	1.392(8)	this work
Ni(3)	2.157(2)	1.693(6)	1.403(8)	this work
with (*S*)-**2**				
Ni(1)	2.1575(10)	1.699(3)	1.391(0)	this work
Ni(2)	2.165(1)	1.712(3)	1.375(5)	this work
Ni(3)	2.158(1)	1.697(3)	1.393(5)	this work
with (*S*)-**3**				
Ni(1)	2.1643(17)	1.709(8)	1.380(10)	this work
Ni(2)	2.1608(17)	1.700(8)	1.377(10)	this work
Ni(3)	2.1606(17)	1.702(8)	1.382(10)	this work
Ni(4)	2.1673(18)	1.709(8)	1.368(10)	this work
Ni(5)	2.1555(18)	1.697(8)	1.387(10)	this work

[a] As n-Bu_4N^+ salt. [b] As *N*,*N*-dimethylpyrrolidinium salt.

alternating along the *b* axis with essentially neutral oxidized complex Ni(3).

The mixed-valence salt with the ^{t}Bu cation, (*S*)-**2**, also adopts a 1:3 stoichiometry with a formulation which includes two solvent molecules, that is, $[(S)\text{-}\mathbf{2}][Ni(dmit)_2]_3\cdot(CH_3CN)_2$. It crystallizes in the orthorhombic system, chiral space group $P2_12_12_1$, with three $[Ni(dmit)_2]$ complexes in general position, together with one (*S*)-**2** cation and two CH_3CN molecules (Figure 3).

Note that specifically with this chiral cation the localization of the NMe_3 group is not straightforward, as the isosteric *tert*-butyl and trimethylammonium groups can be confused during structure resolution (Scheme 1). The choice was made to keep the (*S*) chirality of the cation, affording a (*S*)-**2** cation with, as expected N^+−Me bonds notably shorter than the C−Me bonds in the ^{t}Bu group. The cations organize together with the acetonitrile molecules in the *ab* plane (Figure 4), with nitrile groups pointing toward the activated hydrogen atoms of the NMe_3^+ substituents to form a $N^+-CH_3\cdots N\equiv C-CH_3$ hydrogen-bond network, while the methyl groups of the ^{t}Bu substituent are not engaged in any such interactions, confirming the actual cation chirality.

As observed with the first salt, analysis of intramolecular bond lengths within the three independent complexes in $[(S)\text{-}\mathbf{2}][Ni(dmit)_2]_3\cdot(CH_3CN)_2$ (Table 1) indicates that the three complexes do not have the same charge, with Ni(1) and Ni(3) comparable to the neutral $[Ni(dmit)_2]^0$ complex while Ni(2) looks essentially as the monoanionic $[Ni(dmit)_2]^-$ complex. Within the layers, the molecules are organized onto trimerized stacks (Figure 5), with the less oxidized radical anion Ni(2) species interspersed between the two oxidized, essentially neutral complexes Ni(1) and Ni(3), giving rise to three different overlap interactions, two essentially eclipsed ones for Ni(1)−Ni(2) and Ni(2) −Ni(3) defining the trimer, a more distorted one for the Ni(1)−Ni(3) overlap. Calculations of the $\beta_{LUMO-LUMO}$ interaction energies for the three Ni(1)−Ni(2), Ni(2)−Ni(3), and Ni(1)−Ni(3) pairs of $[Ni(dmit)_2]$ com-

dx.doi.org/10.1021/ic300146s | Inorg. Chem. 2012, 51, 7144−7152

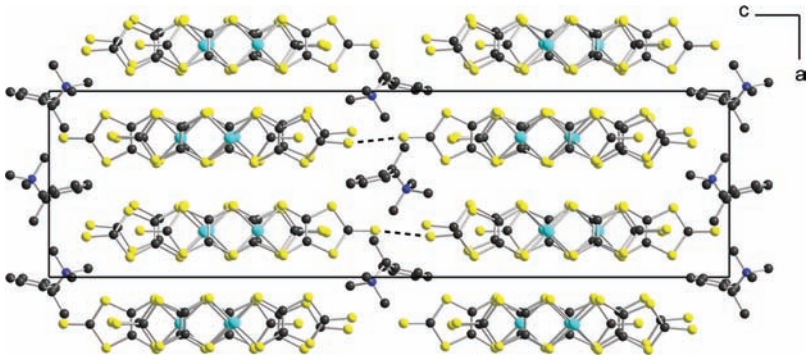

Figure 1. Projection view along the *b* axis of the unit cell of $[(R)\text{-}\mathbf{1}][Ni(dmit)_2]_3$.

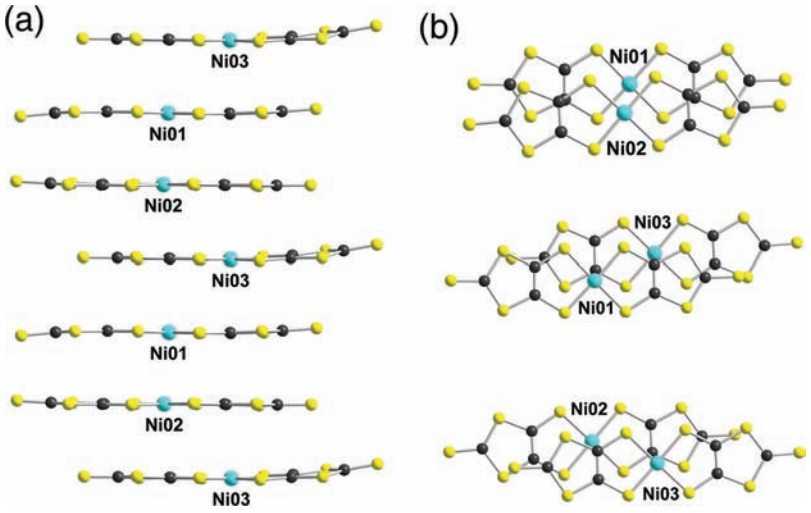

Figure 2. View of the stacks of $[Ni(dmit)_2]$ species (left) together with the intermolecular overlap pattern (right).

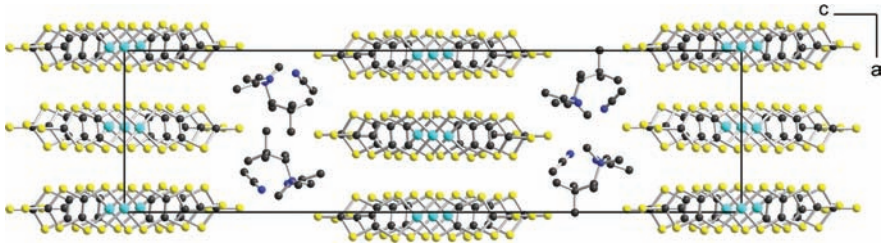

Figure 3. Projection view along the *b* axis of the unit cell of the ^{t}Bu salt, $[(S)\text{-}\mathbf{2}][Ni(dmit)_2]\cdot(CH_3CN)_2$.

Scheme 1

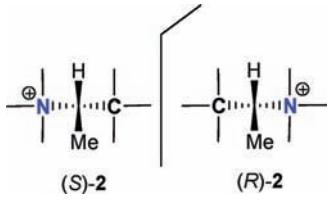

plexes confirm this observation with $\beta_{12} = -0.51$, $\beta_{23} = -0.53$, and $\beta_{13} = -0.03$ eV, respectively.

A side view of dithiolene slabs for both complexes with (R)-**1** and (S)-**2**, taking into account the charge distribution discussed above, is shown in Figure 6, demonstrating that the radical species are only weakly interacting with each other along the *a* direction in $[(R)\text{-}\mathbf{1}][Ni(dmit)_2]_3$, while they are fully isolated from each other by essentially neutral complexes in $[(S)\text{-}\mathbf{2}][Ni(dmit)_2]\cdot(CH_3CN)_2$. This structural analysis is reinforced by the temperature dependence of the magnetic susceptibility of both salts (Figures S1 and S2, Supporting Information), well fitted in the whole temperature range with a Curie–Weiss law for one $S = 1/2$ species, $\chi = \chi_0 + Ng^2\beta^2/3k(T - \theta)$ with for $[(R)\text{-}\mathbf{1}][Ni(dmit)_2]_3$ $\chi_0 = 2.139(8) \times 10^{-3}$ cm^3 mol^{-1}, $g = 2.139(9)$, and $\theta = -1.89(4)$ K and for $[(S)\text{-}\mathbf{2}][Ni(dmit)_2]\cdot(CH_3CN)_2$ $\chi_0 = 0.75(4) \times 10^{-3}$ cm^3 mol^{-1}, $g = 2.131(4)$, and $\theta = -2.41(2)$ K. This behavior indicates that the radical species in both salts are essentially localized, with negligible interactions between trimers. As a consequence, the two salts are semiconducting with a similar room-temperature conductivity, σ_{RT}, of 0.02 S cm^{-1} (Figure 7) together with large activation energies, 0.13 and 0.17 eV for $[(R)\text{-}\mathbf{1}][Ni(dmit)_2]_3$ and $[(S)\text{-}\mathbf{2}][Ni(dmit)_2]\cdot(CH_3CN)_2$, respectively.

A more complex structure is found with the larger naphthyl cation (S)-**3**, which affords a salt with a rare 2:5 stoichiometry,

dx.doi.org/10.1021/ic300146s | *Inorg. Chem.* 2012, 51, 7144–7152

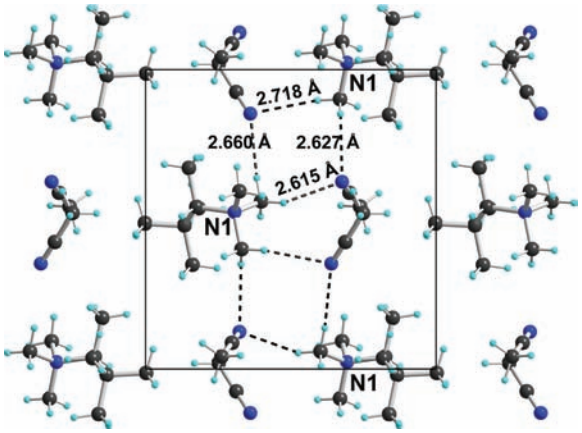

Figure 4. Weak $N^+-CH_3\cdots N\equiv C-CH_3$ hydrogen-bond network between the (*S*)-**2** cation and CH_3CN molecules in $[(S)\text{-}\mathbf{2}][Ni(dmit)_2]_3\cdot(CH_3CN)_2$.

$[(S)\text{-}\mathbf{3}]_2[Ni(dmit)_2]_5\cdot(CH_3CN)_4$. It crystallizes in the triclinic system, space group *P*1, with now five crystallographically independent $[Ni(dmit)_2]$ complexes, two cations, and four solvent (CH_3CN) molecules (Figure 8). Among the five dithiolene complexes, Ni(1) and Ni(4) appear as the less oxidized ones, while Ni(2), Ni(3), and Ni(5) are closer to neutral $[Ni(dmit)_2]^0$. A side view of the stacks (Figure 9) shows an alternation of Ni(1)−Ni(3) dimers and Ni(2)−Ni(4)−Ni(5) trimers along *b*. Again, the charge localization deduced from comparison of intramolecular bond lengths leads to a charge localization illustrated in Figure 9c and confirmed by the temperature dependence of the magnetic susceptibility (Figure S3, Supporting Information). It is well fitted with a Curie−Weiss law for two $S = 1/2$ species, $\chi = \chi_0 + 2Ng^2\beta^2/3k(T-\theta)$, with $\chi_0 = 4.3(1) \times 10^{-3}$ cm^3 mol^{-1}, $g = 2.004(6)$, and $\theta = -0.95$ K. This strong localization leads to a semiconducting behavior ($\sigma_{RT} = 0.028$ S cm^{-1}, $E_{act} = 0.12$ eV, Figure 7) comparable to that observed in the other two salts.

A recurrent behavior is found for those three chiral salts, all characterized with formation of dimers or trimers with two recurrent overlap interactions, described as mode A (small lateral shift with large overlap interaction) and mode B (long longitudinal displacement with small associated overlap interaction) in many solid crossing column structures, as found in the prototypical $(NMe_4)[Ni(dmit)_2]_2$.[33] The main

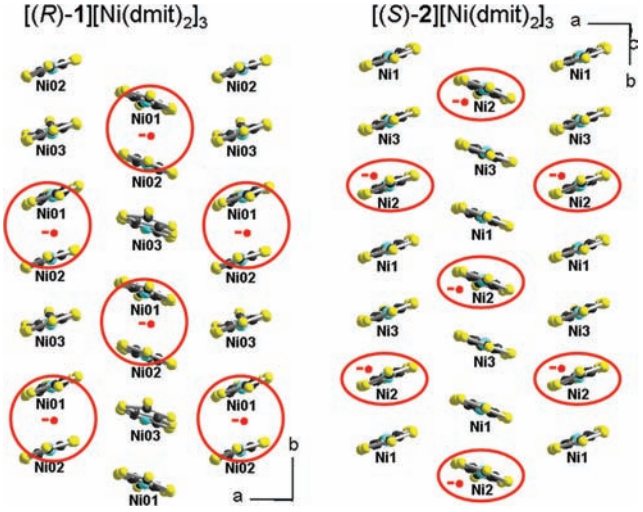

Figure 6. View of the slab built out of $[Ni(dmit)_2]$ species in $[(R)\text{-}\mathbf{1}][Ni(dmit)_2]_3$ (left) and $[(S)\text{-}\mathbf{2}][Ni(dmit)_2]\cdot(CH_3CN)_2$ (right) with charge repartition deduced from comparison of intramolecular bond distances.

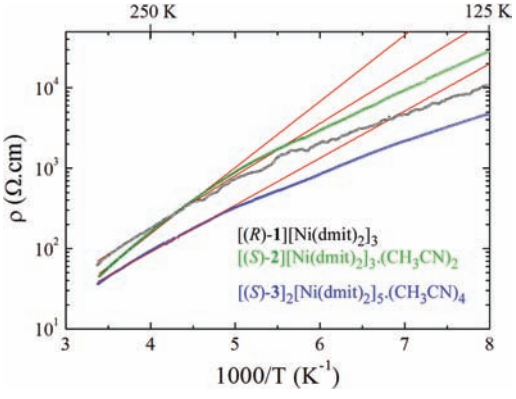

Figure 7. Temperature dependence of the resistivity of the three salts. Red line is a model in the high-temperature regime with $\rho = \rho_0 \exp(E_{act}/kT)$.

difference with the reported conducting salts is the unusual stoichiometries (1:3, 2:5) encountered here which can potentially be attributed to the larger size of the cation and, most importantly, the large number of crystallographically

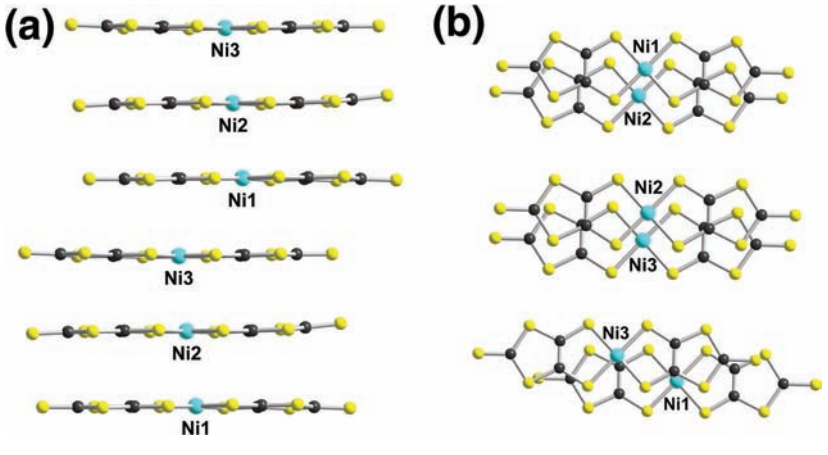

Figure 5. Detail of the trimerized stacks (left) and overlap patterns within stacks (right) in $[(S)\text{-}\mathbf{2}][Ni(dmit)_2]\cdot(CH_3CN)_2$.

dx.doi.org/10.1021/ic300146s | *Inorg. Chem.* 2012, 51, 7144−7152

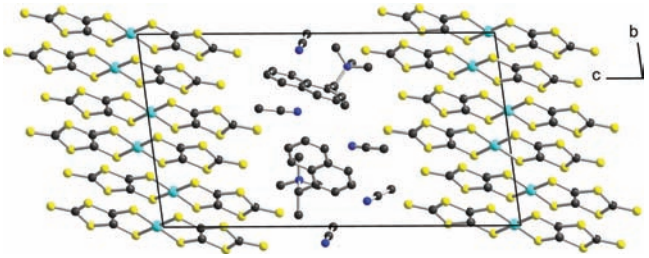

Figure 8. Projection view along the *a* axis of the unit cell of $[(S)\text{-}\mathbf{3}]_2[Ni(dmit)_2]_5\cdot(CH_3CN)_4$.

independent $[Ni(dmit)_2]$ complexes. Indeed, with 3 or even 5 different complexes we systematically observe a strong charge localization of the radical anion species $[Ni(dmit)_2]^{-\bullet}$, interspersed with oxidized, essentially neutral complexes $[Ni(dmit)_2]^0$. This recurrent charge localization is at the origin of the systematic semiconducting behavior of the salts. In other words, the main effect of introduction of chiral cations appears here to be loss of inversion centers, favoring a large number of crystallographically independent complexes with different redox states and the associated charge localization.

A comparison with the analogous racemic $[Ni(dmit)_2]$ salts would be particularly interesting to shed light on this point. Our attempts to grow crystals by the same electrocrystallization experiments with (*rac*)-**1**, (*rac*)-**2**, or (*rac*)-**3** cation afforded contrasted results. We were not able to grow a crystal of proper quality with the $[(rac)\text{-}\mathbf{1},PF_6]$ mixture, while the $[(rac)\text{-}\mathbf{3},PF_6]$ electrolyte afforded systematically the enantiopure salt described above with either (*R*)-**3** or (*S*)-**3**, a first and remarkable example of racemic resolution in electrocrystallization experiments.

On the other hand, the ^{t}Bu derivative, as racemic mixture, $[(rac)\text{-}\mathbf{2},PF_6]$, afforded two different phases, depending on the temperature of the electrocrystallization experiment, a monoclinic phase (space group *Pn*) with electrocrystallizations conducted at room temperature (~20 °C) and a triclinic phase (space group *P*−1) at higher temperatures (40 °C). In the high-temperature triclinic phase (space group *P*−1) the salt formulated as $[(rac)\text{-}\mathbf{2}][Ni(dmit)_2]_3\cdot(CH_3CN)_2$ adopts the 1:3 stoichiometry (Figure 10), with two complexes [Ni(1) and Ni(3)] on inversion centers and, on general positions, two complexes [Ni(2) and Ni(4)] and one cation, with the (*R*)-**2** and (*S*)-**2** enantiomers disordered on the same site (See scheme 1). Again, the complexes organize into trimers $[Ni(2)-Ni(1)-Ni(2)]^{-1}$ and $[Ni(4)-Ni(3)-Ni(4)]^{-1}$ (Figure S4, Supporting Information) with, based on intramolecular bond lengths (Table S1, Supporting Information), central inversion-centered radical anion complexes [Ni(1), Ni(3)] sandwiched between two essentially neutral complexes. These trimers form slabs separated by the cation layers.

In the room-temperature monoclinic phase with the same formulation, $[(rac)\text{-}\mathbf{2}][Ni(dmit)_2]_3\cdot(CH_3CN)_2$, three crystallographically independent $[Ni(dmit)_2]$ moieties are located in a general position, together with one cation and two disordered CH_3CN molecules (Figure 11). The $[Ni(dmit)_2]$ complexes are associated into [Ni(1)−Ni(2)−Ni(3)] trimers (Figure S5, Supporting Information), and intramolecular bond lengths (Table S1) within the three complexes indicate that the central Ni(2) complex is less oxidized than the two others, with this radical anion sandwiched between two neutral complexes, as already observed in the two different trimers of the triclinic phases. Hence, the two racemic structures are closely related and both characterized by formation of trimers with the radical anion diluted between essentially neutral, oxidized $[Ni(dmit)_2]^0$ complexes (Figures S6 and S7, Supporting Information).

In conclusion, we described here the first examples of conducting *and* chiral metal dithiolene salts. In such compounds, chirality can be introduced either on the dithiolene complex itself or on the counterion. We explored the second possibility with introduction of chiral, enantiopure cations as electrolyte in the electrocrystallization experiments. Partial oxidation of the radical $[Ni(dmit)_2]^-$ in the presence of three different enantiopure cations derived from chiral primary amines leads to formation of mixed-valence salts with unusual stoichiometries and a cation/complex ratio of 1:3 or 2:5. Their semiconducting character finds its origin in a strong electron localization, favored by the large number of crystallographically independent $[Ni(dmit)_2]$ complexes in these chiral structures and their association into weakly interacting dimeric or trimeric motifs. Because of their chiral character, the absence of

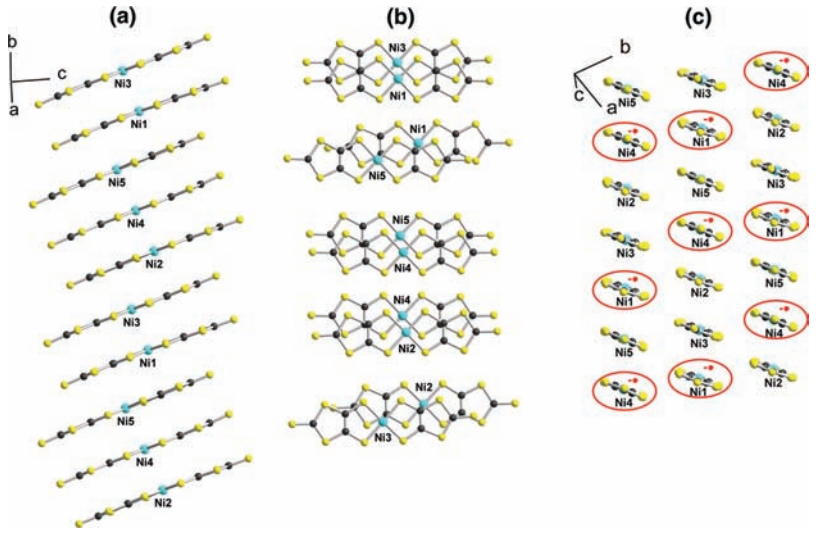

Figure 9. Structure of $[(S)\text{-}\mathbf{3}]_2[Ni(dmit)_2]_5\cdot(CH_3CN)_4$ with (a) detail of the alternating dimer and trimer structure of the stack of $[Ni(dmit)_2]$ moieties, (b) the overlap patterns between molecules, and (c) the charge repartition deduced from comparison of intramolecular bond distances.

dx.doi.org/10.1021/ic300146s | *Inorg. Chem.* 2012, 51, 7144−7152

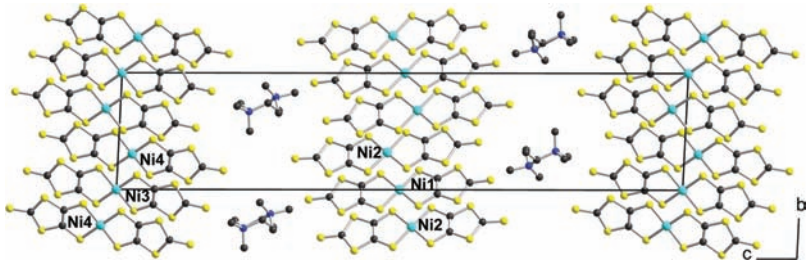

Figure 10. Projection view (along the *a* axis) of the unit cell of the triclinic phase of $[(rac)\text{-}\mathbf{2}][Ni(dmit)_2]\cdot(CH_3CN)_2$. Solvent molecules were omitted.

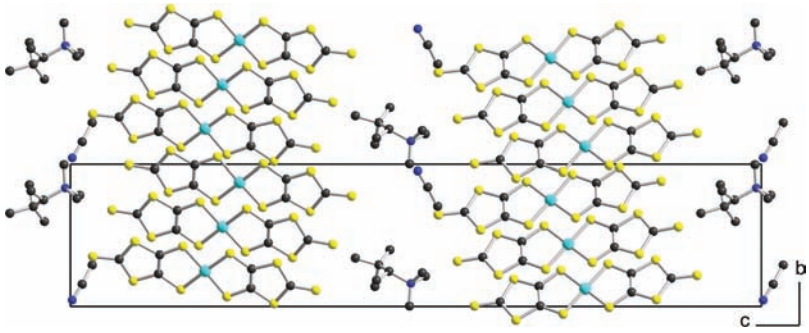

Figure 11. Projection view (along the *a* axis) of the unit cell of the monoclinic phase of $[(rac)\text{-}\mathbf{2}][Ni(dmit)_2]\cdot(CH_3CN)_2$.

Table 3. Electrocrystallization Conditions

electrolyte nature	electrolyte (mg)	TBA[Ni(dmit)$_2$] (mg)	current (μA)	T (°C)	phase obtained
$[(R)\text{-}\mathbf{1}]PF_6$	11.1	3.7	0.5	20(1)	$[(R)\text{-}\mathbf{1}][Ni(dmit)_2]_3$
$[(S)\text{-}\mathbf{2}]PF_6$	14.6	5.0	0.5	20(1)	$[(S)\text{-}\mathbf{2}][Ni(dmit)_2]_3\cdot(CH_3CN)_2$
$[(S)\text{-}\mathbf{3}]PF_6$	23.3	5.9	1	20(1)	$[(S)\text{-}\mathbf{3}]_2[Ni(dmit)_2]_5\cdot(CH_3CN)_4$
$[rac\text{-}\mathbf{2}]PF_6$	19.4	5.5	0.5	20(1)	$[rac\text{-}\mathbf{2}][Ni(dmit)_2]_3\cdot(CH_3CN)_2$ monoclinic phase (SG *Pn*)
$[rac\text{-}\mathbf{2}]PF_6$	30.3	10.7	0.5	40(1)	$[rac\text{-}\mathbf{2}][Ni(dmit)_2]_3\cdot(CH_3CN)_2$ triclinic phase (SG *P*−1)
$[rac\text{-}\mathbf{3}]PF_6$	26.4	4.5	0.5	20(2)	$[(S)\text{-}\mathbf{3}]_2[Ni(dmit)_2]_5\cdot(CH_3CN)_4$ or $[(R)\text{-}\mathbf{3}]_2[Ni(dmit)_2]_5\cdot(CH_3CN)_4$

inversion centers in the chiral salts could be a rationale for this behavior. Racemic salts with the same cations were obtained only with difficulty, and those isolated with the *tert*-butyl-containing (*rac*)-**2** cation afforded similar trimerized structures. We finally believe that the complex structures obtained here with chiral cations could be primarily due to their larger size, when compared with classical closed-shell cations as $(NH_xMe_{4-x})^+$ (x = 0−3) or $(MMe_xEt_{4-x})^+$ (M = N, P, As, Sb; x = 0−4), which favor recurrent 1:2 stoichiometry and highly conducting character.[18] Other stoichiometries (1:3, 2:5) were indeed reported only with much larger cations such as $(MePh_3P)^+$,[34] $(BzMe_3P)^+$,[35] Ph_4P^+,[36] acridinium,[37] phenazinium,[38] or $[(NH_4)(18\text{-crown-}6)]^+$.[39] On the basis of this assumption, smaller and still chiral cations could be considered in the future, such as *N*-methyl oxazolinium[40] or *N*-methyl thiazolinium cations.[41] Besides, numerous possibilities are also offered by a direct functionalization of the dithiolene complex itself with chiral substituents.[23−25]

EXPERIMENTAL SECTION

Syntheses. The trimethylammonium salts were prepared as previously described for the iodide $[(S)\text{-}\mathbf{1},I]$.[28] The enantiopure or racemic amine is reacted in MeOH at reflux overnight in the presence of MeI (7 equiv) and $NaHCO_3$ (4 equiv). After cooling, the solvent is evaporated under vacuum and the residue extracted with CH_2Cl_2. The filtered solution of the iodide is evaporated; the residue redissolved in MeOH and HPF_6 (60% in H_2O, 1 equiv) is added. Recrystallization of the precipitated PF_6^- salt in hot MeOH leads to the hexafluorophosphates as white crystals.

$[(R)\text{-}\mathbf{1}]PF_6$. Yield: 63%. ^{1}H NMR (d_6-DMSO, TMS, 300 MHz): δ 1.70 (3H, d, CH_3), 2.96 (9H, s, CH_3), 4.74 (1H, q, CH), 7.47−7.60 (5H, m, Ar). ^{13}C NMR (d_6-DMSO, TMS, 300 MHz): δ 14.27 (CH_3), 50.22 (CH_3), 72.34 (CH), 128.62 (CH Ar), 129.94 (CH Ar), 130.21 (CH Ar), 133.26 (C Ar). Anal. Calcd for $C_{11}H_{18}NPF_6$: C, 42.8; H, 5.6; N, 4.5. Found: C, 42.57; H, 5.86; N, 4.72.

$[(S)\text{-}\mathbf{2}]PF_6$. Yield: 20%. ^{1}H NMR (d_6-DMSO, TMS, 300 MHz): δ 1.13 (9H, s, CH_3), 1.31−1.35 (3H, m, CH_3), 3.09 (9H, s, CH_3), 3.46 (1H, q, CH). ^{13}C NMR (d_6-DMSO, TMS, 300 MHz): δ 12.32 (CH_3), 29.05 (CH_3), 36.29 (CH_2), 52.99 (CH_3), 77.84 (CH). Anal. Calcd for $C_9H_{12}NPF_6$: C, 37.5; H, 7.3; N, 4.8. Found: C, 37.55; H, 7.60; N, 4.64.

$[(S)\text{-}\mathbf{3}]PF_6$. Yield: 72%. ^{1}H NMR (d_6-DMSO, TMS, 300 MHz): δ 1.83 (3H, d, CH_3), 3.03 (9H, s, CH_3), 5.74 (1H, q, CH), 7.59−7.71 (3H, m, Ar), 7.94 (1H, d, Ar), 8.05 (1H, d, Ar), 8.11 (1H, d, Ar), 8.56 (1H, d, Ar). ^{13}C NMR (d_6-DMSO, TMS, 300 MHz): δ 15.60 (CH_3), 50.45 (CH_3), 65.94 (CH), 123.13 (Ar), 125.14 (Ar), 126.07 (Ar), 127.22 (Ar), 128.29 (Ar), 129.06 (Ar), 129.63 (Ar), 130.68 (Ar), 132.02 (Ar), 133.36 (Ar). Anal. Calcd for $C_{15}H_{20}NPF_6$: C, 50.3; H, 5.4; N, 3.9. Found: C, 48.79; H, 5.49; N, 3.86.

$[(rac)\text{-}\mathbf{1}]PF_6$. Yield: 81%. ^{1}H NMR (d_6-DMSO, TMS, 300 MHz): δ 1.70 (3H, d, CH_3), 2.96 (9H, s, CH_3), 4.74 (1H, q, CH), 7.47−7.60 (5H, m, Ar). ^{13}C NMR (d_6-DMSO, TMS, 300 MHz): δ 14.27 (CH_3), 50.22 (CH_3), 72.34 (CH), 128.62 (CH Ar), 129.94 (CH Ar), 130.21 (CH Ar), 133.26 (C Ar). Anal. Calcd for $C_{11}H_{18}NPF_6$: C, 42.8; H, 5.6; N, 4.5. Found: C, 42.71; H, 5.65; N, 4.48.

$[(rac)\text{-}\mathbf{2}]PF_6$. Yield: 85%. ^{1}H NMR (d_6-DMSO, TMS, 300 MHz): δ 1.13 (9H, s, CH_3), 1.31−1.35 (3H, m, CH_3), 3.09 (9H, s, CH_3), 3.46 (1H, q, CH). ^{13}C NMR (d_6-DMSO, TMS, 300 MHz): δ 12.32 (CH_3),

dx.doi.org/10.1021/ic300146s | *Inorg. Chem.* 2012, 51, 7144−7152

Table 4. Crystallographic Data[a]

compound	[(*R*)-**1**][Ni(dmit)$_2$]$_3$	[(*S*)-**2**][Ni(dmit)$_2$]$_3$·(CH$_3$CN)$_2$	[(*S*)-**3**]$_2$[Ni(dmit)$_2$]$_5$·(CH$_3$CN)$_4$	[(*rac*)-**2**] [Ni(dmit)$_2$]$_3$·(CH$_3$CN)$_2$	[(*rac*)-**2**][Ni(dmit)$_2$]$_3$·(CH$_3$CN)$_2$
formula	$C_{29}H_{18}NNi_3S_{30}$	$C_{31}H_{28}N_3Ni_3S_{30}$	$C_{68}H_{52}$ $N_6Ni_5S_{50}$	$C_{27}H_{22}NNi_3S_{30}$	$C_{29}H_{25}N_2Ni_3S_{30}$
fw (g·mol^{-1})	1518.37	1580.49	2849.71	1498.39	1539.44
cryst color	black	black	black	black	black
cryst size (mm)	0.27 × 0.10 × 0.083	0.45 × 0.23 × 0.07	0.54 × 0.46 × 0.07	0.35 × 0.12 × 0.07	0.32 × 0.24 × 0.06
cryst syst	orthorhombic	orthorhombic	triclinic	triclinic	monoclinic
space group	$P2_12_12_1$	$P2_12_12_1$	$P1$	$P-1$	Pn
T (K)	150(2)	150(2)	150(2)	150(2)	150(2)
a (Å)	11.1810(7)	11.2264(9)	8.8577(8)	7.3392(12)	7.3491(6)
b (Å)	11.2057(8)	11.5591(9)	12.8475(12)	8.8475(13)	8.8399(7)
c (Å)	41.036(2)	43.063(3)	23.445(2)	43.122(7)	43.054(3)
α (deg)	90.0	90.0	81.282(4)	92.729(4)	90.0
β (deg)	90.0	90.0	82.505(4)	91.442(5)	91.682(2)
γ (deg)	90.0	90.0	78.952(4)	90.047(4)	90.0
V (Å^3)	5141.4(6)	5588.2(8)	2574.1(4)	2796.0(8)	2795.8(4)
Z	4	4	1	2	2
D_{calcd} (g·cm^{-3})	1.962	1.879	1.838	1.779	1.829
μ (mm^{-1})	2.337	2.155	1.957	2.147	2.150
total reflns	37 826	33 566	44 874	43 976	21 049
abs corr	multiscan	multiscan	multiscan	multiscan	multiscan
T_{min}, T_{max}	0.760, 0.824	0.557, 0.860	0.361, 0.872	0.741, 0.860	0.544, 0.879
unique reflns	11 463	12 550	18 808	12 753	10 950
R_{int}	0.0518	0.0375	0.0335	0.0409	0.0330
unique reflns ($I > 2\sigma(I)$)	8497	10 596	14 622	10 454	9408
refined params	572	606	1174	554	572
R_1 ($I > 2\sigma(I)$)	0.0384	0.0293	0.0318	0.0495	0.0524
wR_2 (all data)	0.1239	0.0927	0.1184	0.1459	0.1638
goodness-of-fit	1.027	1.107	1.102	1.070	1.088
residual density (e·Å^{-3})	0.831, −1.010	0.928, −0.979	0.542, −0.750	1.525, −0.924	0.806, −1.480

[a] $R_1 = \Sigma||F_o| - |F_c||/\Sigma|F_o|$. $wR_2 = [\Sigma w(F_o^2 - F_c^2)^2/\Sigma wF_o^4]^{1/2}$.

29.05 (CH$_3$), 36.29 (CH$_2$), 52.99 (CH$_3$), 77.84 (CH). Anal. Calcd for $C_9H_{12}NPF_6\cdot(H_2O)_4$: C, 30.78; H, 5.74; N, 3.99. Found: C, 29.97; H, 6.10; N, 3.90.

[(*rac*)-**3**]PF$_6$. Yield: 81%. ^{1}H NMR (DMSO): δ 1.83 (3H, d, CH$_3$), 3.03 (9H, s, CH$_3$), 5.75 (1H, q, CH), 7.59−7.72 (3H, m, Ar), 7.94 (1H, d, Ar), 8.05 (1H, d, Ar), 8.11 (1H, d, Ar), 8.56 (1H, d, Ar). ^{13}C NMR (DMSO): δ 15.60 (CH$_3$), 50.45 (CH$_3$), 65.94 (CH), 123.13 (Ar), 125.14 (Ar), 126.07 (Ar), 127.22 (Ar), 128.29 (Ar), 129.06 (Ar), 129.63 (Ar), 130.68 (Ar), 132.02 (Ar), 133.36 (Ar). Anal. Calcd for $C_{15}H_{20}NPF_6$: C, 50.3; H, 5.4; N, 3.9. Found: C, 50.07; H, 5.53; N, 3.76.

Electrocrystallization Experiments. They were conducted in two-compartment cells equipped with Pt electrodes (diameter 1 mm, length 2 cm) with the hexafluorophosphate ammonium salt dissolved in CH$_3$CN (10 mL) as electrolyte and nBu$_4$N[Ni(dmit)$_2$] as electroactive compound in the anodic compartment. Details are collected in Table 3 for the different salts.

X-ray Diffraction Studies. Single crystals were taken in a loop in oil and put directly under the N$_2$ stream at 150 K to avoid solvent losses. Data were collected on a Bruker SMART II diffractometer with graphite-monochromated Mo Kα radiation (λ = 0.71073 Å). Structures were solved by direct methods (SHELXS-97, SIR97)[42] and refined (SHELXL-97) by full-matrix least-squares methods,[43] as implemented in the WinGX software package.[44] Absorption corrections were applied. Hydrogen atoms were introduced at calculated positions (riding model), included in structure factor calculations, and not refined. Crystallographic data are summarized in Table 4. A SQUEEZE procedure for two disordered CH$_3$CN molecules was applied for the triclinic phase of [(*rac*)-**2**][Ni(dmit)$_2$]$_3$ as well as for one of two CH$_3$CN molecules in the monoclinic phase of [(*rac*)-**2**][Ni(dmit)$_2$]$_3$.

Magnetic Properties. Magnetic susceptibility measurements were obtained from a Quantum Design SQUID magnetometer MPMS-XL. This magnetometer works between 1.8 and 400 K for dc applied fields ranging from −5 to 5 T. Measurements were performed on polycrystalline samples of [(*R*)-**1**][Ni(dmit)$_2$]$_3$ (4.7 mg), [(*S*)-**2**][Ni(dmit)$_2$]$_3$·(CH$_3$CN)$_2$ (3.8 mg), and [(*S*)-**3**]$_2$[Ni(dmit)$_2$]$_5$·(CH$_3$CN)$_4$ (4.6 mg). Magnetic data were corrected for the sample holder and diamagnetic contributions.

Theoretical Calculations. $\beta_{LUMO-LUMO}$ interaction energies were based upon the effective one-electron Hamiltonian of the extended Hückel method,[45] as implemented in the Caesar 1.0 chain of programs.[46] The off-diagonal matrix elements of the Hamiltonian were calculated according to the modified Wolfsberg−Helmholz formula.[47] All valence electrons were explicitly taken into account in the calculations, and the basis set consisted of double-ζ Slater-type orbitals for C, S, and Ni and single-ζ Slater-type orbitals for H.

■ ASSOCIATED CONTENT

Supporting Information

CIF files for the five reported X-ray crystal structures. Temperature dependence of the magnetic susceptibility of the three chiral salts [(*R*)−**1**][Ni(dmit)$_2$]$_3$, [(*S*)−**2**][Ni(dmit)$_2$]$_3$·(CH$_3$CN)$_2$, and [(*S*)−**3**]$_2$[Ni(dmit)$_2$]$_5$·(CH$_3$CN)$_4$. Table of intramolecular bond distances and structural descriptions for the two racemic salts [(*rac*)−**2**][Ni(dmit)$_2$]$_3$·(CH$_3$CN)$_2$. This material is available free of charge via the Internet at http://pubs.acs.org.

dx.doi.org/10.1021/ic300146s | Inorg. Chem. 2012, 51, 7144−7152

AUTHOR INFORMATION

Corresponding Author

*E-mail: marc.fourmigue@univ-rennes1.fr.

Notes

The authors declare no competing financial interest.

ACKNOWLEDGMENTS

We thank the CDIFX (Rennes) for access to the X-ray diffraction facilities and the ANR (France) for financial support through project no. ANR-08-BLAN-0140-02.

REFERENCES

(1) (a) Krstic, V.; Roth, S.; Burghard, M.; Kern, K.; Rikken. *J. Chem. Phys.* **2002**, *117*, 11315. (b) Krstic, V.; Rikken, G. L. J. A. *Chem. Phys. Lett.* **2002**, *364*, 51.

(2) Avarvari, N.; Wallis, J. D. *J. Mater. Chem.* **2009**, *19*, 4061.

(3) (a) Coronado, E.; Galán-Mascarós, J. R. *J. Mater. Chem.* **2005**, *15*, 66. (b) Amabilino, D. B.; Veciana, J. *Top. Curr. Chem.* **2006**, *265*, 253.

(4) Dunitz, J. D.; Karrer, A.; Wallis, J. D. *Helv. Chim. Acta* **1986**, *69*, 69.

(5) (a) Yang, S.; Brooks, A. C.; Martin, L.; Day, P.; Li, H.; Horton, P.; Male, L.; Wallis, J. D. *CrystEngComm* **2009**, *11*, 993. (b) Wallis, J. D.; Griffiths, J. P. *J. Mater. Chem.* **2005**, *15*, 347. Brown, R. J.; Brooks, A. C.; Griffiths, J.-P.; Vital, B.; Day, P.; Wallis, J. D. *Org. Biomol. Chem.* **2007**, *5*, 3172.

(6) (a) Karrer, A.; Wallis, J. D.; Dunitz, J. D.; Hilti, B.; Mayer, C. W.; Bürkle, M.; Pfeiffer, J. *Helv. Chim. Acta* **1987**, *70*, 942. (b) Matsumiya, S.; Izuoka, A.; Sugawara, T.; Taruishi, T.; Kawada, Y.; Tokumoto, M. *Bull. Chem. Soc. Jpn.* **1993**, *66*, 1949.

(7) Galan-Mascaros, J. R.; Coronado, E.; Goddard, P. A.; Singleton, J.; Coldea, A. I.; Wallis, J. D.; Coles, S. J.; Alberola, A. *J. Am. Chem. Soc.* **2010**, *132*, 9271.

(8) (a) Réthoré, C.; Fourmigué, M.; Avarvari, N. *Chem. Commun.* **2004**, 1384. (b) Réthoré, C.; Madalan, A.; Fourmigué, M.; Canadell, E.; Lopes, E.; Almeida, M.; Clérac, R.; Avarvari, N. *New J. Chem.* **2007**, *31*, 1468. (c) Réthoré, C.; Fourmigué, M.; Avarvari, N. *Tetrahedron* **2005**, *61*, 10935.

(9) Réthoré, C.; Avarvari, N.; Canadell, E.; Auban-Senzier, P.; Fourmigué, M. *J. Am. Chem. Soc.* **2005**, *127*, 5748. Madalan, A. M.; Réthoré, C.; Fourmigué, M.; Canadell, E.; Lopes, E. B.; Almeida, M.; Auban-Senzier, P.; Avarvari, N. *Chem.—Eur. J.* **2010**, *16*, 528.

(10) (a) Saad, A.; Barrière, F.; Levillain, E.; Vanthuyne, N.; Jeannin, O.; Fourmigué, M. *Chem.—Eur. J.* **2010**, *16*, 8020. (b) Saad, A.; Jeannin, O.; Fourmigué, M. *New J. Chem.* **2011**, *35*, 1004. (c) Saad, A.; Jeannin, O.; Fourmigué, M. *Tetrahedron* **2011**, *67*, 3820. (d) Saad, A.; Jeannin, O.; Fourmigué, M. *CrystEngCommun* **2010**, *12*, 3866.

(11) (a) Martin, L.; Turner, S. S.; Day, P.; Mabbs, F. E.; McInnes, E. J. L. *Chem. Commun.* **1997**, 1367. (b) Martin, L.; Turner, S. S.; Day, P.; Malik, K. M. A.; Coles, S. J.; Hursthouse, M. B. *Chem. Commun.* **1999**, 513. (c) Martin, L.; Turner, S. S.; Day, P. *Synth. Met.* **1999**, *102*, 1638.

(12) (a) Gomez-Garcia, C. J.; Coronado, E.; Curreli, S.; Gimenez-Saiz, C.; Deplano, P.; Mercuri, M. L.; Pilia, L.; Serpe, A.; Faulmann, C.; Canadell, E. *Chem. Commun.* **2006**, 4931. (b) Coronado, E.; Curreli, S.; Giménez-Saiz, C.; Gómez-García, C. J.; Deplano, P.; Mercuri, M. L.; Serpe, A.; Pilia, L.; Faulmann, C.; Canadell, E. *Inorg. Chem.* **2007**, *46*, 4444.

(13) Chmel, N. P.; Clarkson, G. J.; Troisi, A.; Turner, S. S.; Scott, P. *Inorg. Chem.* **2011**, *50*, 4039.

(14) Coronado, E.; Galan-Mascaros, J. R.; Gomez-Garcia, C. J.; Murcia-Martinez, A.; Canadell, E. *Inorg. Chem.* **2004**, *43*, 8072.

(15) Clemente-Leon, M.; Coronado, E.; Gomez-Garcıa, C. J.; Soriano-Portillo, A.; Constant, S.; Frantz, R.; Lacour, J. *Inorg. Chim. Acta* **2007**, *360*, 955.

(16) (a) Brezgunova, M.; Shin, K. S.; Auban-Senzier, P.; Jeannin, O.; Fourmigué, M. *Chem. Commun.* **2010**, 3226. (b) Shin, K.-S.; Brezgunova, M.; Jeannin, O.; Roisnel, T.; Camerel, F.; Auban-Senzier, P.; Fourmigué, M. *Cryst. Growth Design* **2011**, *11*, 5337.

(17) (a) Martin, L.; Day, P.; Akutsu, H.; Yamada, J.-i.; Nakatsuji, S.-i.; Clegg, W.; Harrington, R. W.; Horton, P. N.; Hursthouse, M. B.; McMillan, P.; Firth, S. *CrystEngComm* **2007**, *9*, 865. (b) Martin, L.; Day, P.; Horton, P.; Nakatsuji, S.-i.; Yamada, J.-i.; Akutsu, H. *J. Mater. Chem.* **2010**, *20*, 2738.

(18) Kato, R. *Chem. Rev.* **2004**, *104*, 5319.

(19) Brossard, L.; Ribault, M.; Bousseau, M.; Valade, L.; Cassoux, P. *C. R. Acad. Sci. Ser. II* **1986**, *302*, 205.

(20) Kobayashi, A.; Kim, H.; Sasaki, Y.; Kato, R.; Kobayashi, H.; Moriyama, S.; Noshio, Y.; Kajita, K.; Sasaki, W. *Chem. Lett.* **1987**, 1819.

(21) (a) Kobayashi, A.; Kobayashi, H.; Miyamoto, A.; Kato, R.; Clark, R. A.; Underhill, A. E. *Chem. Lett.* **1991**, 2163. (b) Kobayashi, H.; Bun, K.; Naito, T.; Kato, R.; Kobayashi, A. *Chem. Lett.* **1992**, 1909. (c) Kato, R.; Kashimura, Y.; Aonuma, S.; Hanasaki, N.; Tajima, H. *Solid State Commun.* **1998**, *105*, 561. (d) Kato, R.; Tajima, N.; Tamura, M.; Yamaura, J.-I. *Phys. Rev. B* **2002**, *66*, 020508.

(22) (a) Itou, T.; Oyamada, A.; Maegawa, S.; Tamura, M.; Kato, R. *Phys. Rev. B* **2008**, *77*, 104413. (b) Yamashita, M.; Nakata, N.; Senshu, Y.; Nagata, M.; Yamamoto, H. M.; Kato, R.; Shibauchi, T.; Matsuda, Y. *Science* **2010**, *328*, 1246. (c) Itou, T.; Oyamada, A.; Maegawa, S.; Kato, R. *Nature Physics* **2010**, *6*, 673. (d) Yamashita, S.; Yamamoto, T.; Nakazawa, Y.; Tamura, M.; Kato, R. *Nat. Commun.* **2011**, *2*, 275. (e) Itou, T.; Yamashita, K.; Nishiyama, M.; Oyamada, A.; Maegawa, S.; Kubo, K.; Kato, R. *Phys. Rev. B* **2011**, *84*, 094405.

(23) Kisch, H.; Eisen, B.; Dinnebier, R.; Shankland, K.; David, W. I. F.; Knoch, F. *Chem.—Eur. J.* **2001**, *7*, 738.

(24) Marshall, K. L.; Schudel, S.; Lippa, I. A. *Proc. SPIE. Int. Soc. Opt. Eng.* **2004**, *52B*, 201.

(25) Perochon, R.; Poriel, C.; Jeannin, O.; Piekara-Sady, L.; Fourmigué, M. *Eur. J. Inorg. Chem.* **2009**, 5413.

(26) This chiral cation was recently used for chirality transfer: (a) Clemente-Leon, M.; Coronado, E.; Dias, J. C.; Soriano-Portillo, A.; Willett, R. D. *Inorg. Chem.* **2008**, *47*, 6458. (b) El-Hachemi, Z.; Mancini, G.; Ribo, J. M.; Sorrenti, A. *J. Am. Chem. Soc.* **2008**, *130*, 15176.

(27) (a) Underhill, A. E.; Ahmad, M. M. *J. Chem. Soc., Chem. Commun.* **1981**, 67. (b) Valade, L.; Legros, J.-P.; Bousseau, M.; Cassoux, P.; Garbauskas, M.; Interrante, L. V. *J. Chem. Soc., Dalton Trans.* **1985**, 783.

(28) Lacour, J.; Vial, L.; Herse, C. *Org. Lett.* **2002**, *4*, 1351.

(29) Fun, H.-K.; Sivakumar, K.; Zuo, J.-L.; Yao, T.-M.; You, X.-Z. *Acta Crystallogr., Sect.C: Cryst. Struct. Commun* **1996**, *52*, 312.

(30) Mulder, M. J. J.; Kooijman, H.; Spek, A. L.; Haasnoot, J. G.; Reedijk, J. *J. Chem. Cryst.* **2002**, *32*, 347.

(31) Cornelissen, J. P.; Loux, R. L.; Jansen, J.; Haasnoot, J. G.; Reedijk, J.; Horn, E.; Speck, A. L.; Pomarede, B.; Legros, J.-P.; Reefman, D. *J. Chem. Soc., Dalton Trans.* **1992**, 2911.

(32) Kushch, N.; Faulmann, C.; Cassoux, P.; Valade, L.; Malfant, I.; Legros, J.-P.; Bowlas, C.; Errami, A.; Kobayashi, A.; Kobayashi, H. *Mol. Cryst. Liq. Cryst. Sci. Technol., Sect. A* **1996**, *284*, 247.

(33) (a) Kobayashi, A.; Kim, H.; Sasaki, Y.; Kato, R.; Kobayashi, H.; Moriyama, S.; Nishio, Y.; Kajita, K.; Sasaki, W. *Chem. Lett.* **1987**, 1819. (b) Kim, H.; Kobayashi, A.; Sasaki, Y.; Kato, R.; Kobayashi, H. *Chem. Lett.* **1987**, 1799. (c) Kajita, K.; Nishio, Y.; Moriyama, S.; Kato, R.; Kobayashi, H.; Sasaki, W.; Kobayashi, A.; Kim, H.; Sasaki, Y. *Solid State Commun.* **1988**, *65*, 361.

(34) Pullen, A. E.; Lui, H.-L.; Tanner, D. B.; Abboud, K. A.; Reynolds, J. R. *J. Mater. Chem.* **1997**, *7*, 377.

(35) Faulmann, C.; Errami, A.; Donnadieu, B.; Malfant, I.; Legros, J.-P.; Cassoux, P.; Rovira, C.; Canadell, E. *Inorg. Chem.* **1996**, *35*, 3856.

(36) (a) Nakamura, T.; Underhill, A. E.; Coomber, A. T.; Friend, R. H.; Tajima, H.; Kobayashi, A.; Kobayashi, H. *Synth. Met.* **1995**, *70*, 1061. (b) Liu, H. L.; Tanner, D. B.; Pullen, A. E.; Abboud, K. A.; Reynolds, J. R. *Phys. Rev. B* **1996**, *53*, 10557.

(37) Veldhuizen, Y. S. J.; Haasnoot, J. G.; Reedijk, J. *Synth. Met.* **1997**, *86*, 1827.

(38) Veldhuizen, Y. S. J.; Smeets, W. J. J.; Veldman, N.; Spek, A. L.; Faulmann, C.; Auban-Senzier, P.; Jérome, D.; Paulus, P. M.; Haasnoot, J. G.; Reedijk, J. *Inorg. Chem.* **1997**, *36*, 4930.
(39) Akutagawa, T.; Nakamura, T.; Inabe, T.; Underhill, A. E. *Thin Solid Films* **1998**, *331*, 264.
(40) Wasserscheid, P.; Bösmann, A.; Bolm, C. *Chem. Commun* **2002**, 200.
(41) Levillain, J.; Dubant, G.; Abrunhosa, I.; Gulea, M.; Gaumont, A.-C. *Chem. Commun.* **2003**, 2914.
(42) Altomare, A.; Burla, M. C.; Camalli, M.; Cascarano, G.; Giacovazzo, C.; Guagliardi, A.; Moliterni, A. G. G.; Polidori, G.; Spagna, R. *J. Appl. Crystallogr.* **1999**, *32*, 115.
(43) Sheldrick, G. M. *SHELX97-Programs for Crystal Structure Analysis* (Release 97-2); Institüt für Anorganische Chemie, Universität Göttingen: Göttingen, Germany, 1998.
(44) Farrugia, L. J. *J. Appl. Crystallogr.* **1999**, *32*, 837.
(45) Whangbo, M.-H.; Hoffmann, H. *J. Am. Chem. Soc.* **1978**, *100*, 6093.
(46) Ren, J.; Liang, W.; Whangbo, M.-H. *Crystal and Electronic Structure Analysis Using CAESAR*; PrimeColor Software, Inc.: Cary, NC, 1998.
(47) Ammeter, J.; Bürgi, H.-B.; Thibeault, J.; Hoffmann, R. *J. Am. Chem. Soc.* **1978**, *100*, 3686.